applied sciences

MDPI

Article

Performance of the Dual-Chamber Fungal Fuel Cell in Treating Tannery Wastewater

Mohamed S. Mahmoud [1,2], Jian-Hui Wang [1], Yu Shen [1], Zhi-Wei Guo [1], Yan Yang [1], Dao-Chen Zhu [3], Robert W. Peters [4,*], Mohamed K. Mostafa [5] and Ahmed S. Mahmoud [6,7]

1 National Research Base of Intelligent Manufacturing Service, Chongqing Technology and Business University, Chongqing 400067, China; mphdmicro2012@yahoo.com (M.S.M.); jhwang@ctbu.edu.cn (J.-H.W.); shenyu@ctbu.edu.cn (Y.S.); zwguo@ctbu.edu.cn (Z.-W.G.); yyang@ctbu.edu.cn (Y.Y.)
2 Housing and Building National Research Center (HBRC), Sanitary and Environmental Institute (SEI), Cairo 12311, Egypt
3 Biofuels Institute, School of the Environment and Safety Engineering, Jiangsu University, Zhenjiang 212013, China; dczhucn@ujs.edu.cn
4 Department of Civil, Construction, and Environmental Engineering, University of Alabama at Birmingham, Birmingham, AL 35294, USA
5 Faculty of Engineering and Technology, Badr University in Cairo (BUC), Badr 11829, Egypt; m_khaled@buc.edu.eg
6 Scientific Research Development Unit, Egyptian Russian University (ERU), Badr 11829, Egypt; ahmed-said@eru.edu.eg
7 Institute of Environmental Studies, Arish University, Al Arish 45511, Egypt
* Correspondence: rwpeters@uab.edu

Abstract: Fungi are typically expressed as excellent microorganisms that produce extracellular enzymes used in the bioaccumulation phenomenon. In this study, laboratory-scale dual-chamber fungal fuel cells (FFCs) were applied as an alternate approach for the available degradation of complex organic pollutants represented in chemical oxygen demand (COD) and total nitrogen (TN), as well as inorganic pollutants represented as total chromium (Cr), and the generation of bioenergy represented in output voltages (V), power density (PD) and current density (CD), as applied to tannery effluent. *Aspergillus niger* strain, (*A. niger*), which makes up 40% of the fungal population in tannery effluent was examined in a training study for efficient hexavalent chromium bioaccumulation, especially in high concentrations. The trained *A. niger* showed a faster growth rate than the untrained one in broth media containing different loaded chromium concentrations. For an external resistance of 1000 Ω, two FFCs were utilized, one with electrolytic matrices including phosphate buffer solution (PBS) and bicarbonate buffer solution (BBS), and the other without electrolytic matrices, where the energy generation and treatment efficacy of the two dual-chamber FFCs were evaluated for a period of 165 h. At 15 h, the electrolytic FFCs showed a high voltage output of 0.814 V, a power density of 0.097 $mW \cdot m^{-2}$, and a current density of 0.119 mAm^{-2} compared to the non-electrolytic FFC. At 165 h, the electrolytic FFCs showed high removal efficiency percentages for COD, TN, and total Cr of up to 77.9%, 94.2%, and 73%, respectively, compared to the non-electrolytic FFC.

Keywords: tannery wastewater; fungal fuel cell; bioenergy; electrolytic matrices; total chromium; environmental toxicology; climate actions; adsorption isotherm

Citation: Mahmoud, M.S.; Wang, J.-H.; Shen, Y.; Guo, Z.-W.; Yang, Y.; Zhu, D.-C.; Peters, R.W.; Mostafa, M.K.; Mahmoud, A.S. Performance of the Dual-Chamber Fungal Fuel Cell in Treating Tannery Wastewater. *Appl. Sci.* **2023**, *13*, 10710. https://doi.org/10.3390/app131910710

Academic Editor: Ramaraj Boopathy

Received: 25 May 2023
Revised: 21 September 2023
Accepted: 23 September 2023
Published: 26 September 2023

1. Introduction

The industries that process food and leather, and extract oil produce a great deal of wastewater, which has a negative impact on the environment since it contains significant quantities of heavy metals, organic matter, and total dissolved salts (TDS) [1]. The tanning business is a significant sector of the global economy, yet it is also regarded as one of the most heavily polluting sectors [2]. The ancient Egyptians used tanning methods to tan leather for drums, belts, and shoes throughout their history [3]. Throughout the operating

and production phases, the tanning process utilizing chromium salts is efficient, quick, stable, and inexpensive [4,5]. Due to that process, high chromium concentrations remain in the effluent [6]. Since heavy metals (especially chromium), toxic chemicals, chlorides, lime with high levels of dissolved and suspended salts, total organic matter represented by chemical oxygen demand (COD) and biological oxygen demand (BOD), as well as other pollutants, are present in tannery wastewater, it is recognized as a highly contaminated industrial effluent [7,8]. For every ton of hide, 300 kg of chemicals are applied during the tanning process [9]. About 30 to 35 L of effluent are generated using this method for every kilogram of skin or hide handled [10]. This type of wastewater is considered to be a significant challenge in terms of treatment due to high organic loads along with high salt concentrations [11]. Color, low pH values, high concentrations of sodium chloride indicated by TDS, organic components indicated by COD, certain nitrogenous compounds indicated by total nitrogen (TN), and heavy metals represented as Cr^{6+} are the most common features of tannery wastewater during the tanning process [12,13]. The direct release of this wastewater without proper treatment would result in a decline in water quality [14].

Due to the importance of wastewater reuse in the circular economy and green building themes [15], the treatment of tannery wastewater that is produced in large quantities from the tanning industry has become necessary [16].

There are a number of physico-chemical and bio-chemical technologies that have been developed for treating tannery wastewater [17], including thermal techniques [18], advanced chemical oxidations [19,20], coagulation–flocculation [21], ion exchange [22], and membrane techniques [23]. However, these techniques have several limitations, including high operational costs, high chemical consumption, and secondary pollution that need to be addressed using online intelligent management methods [24,25].

Bio-treatment is an another alternative treatment technology that could be considered as an eco-green method. Beside the low cost of biomaterials that have the ability to degrade and absorb a large number of pollutants, it has a number of limitations that can be represented via its slower operation rate and the requirement for continuous monitoring of all operating parameters affecting the biological behavior of pH and nutrients [17]. To obtain successful treatment, the implementation of design parameters and continuous optimization of conditions need to be adjusted as it changes according to microbial growth factors. At the end of this process, the biological mass representing bio-waste materials will increase and in many cases will require post-treatment to ensure that the old biological mass can be reused or dealt with as part of hazardous organic materials.

Bio-materials are considered to be cultures of bacterial species or fungal species that have the ability to degrade organic materials and produce energy. Although limitations exist for the bio-treatment methodology of operational costs, chemical consumption, and secondary pollution compared to other treatment technologies, the methodology is still considered as a unique approach for generating energy from organic materials [26]. Energy is one of the most important gains from wastewater treatment. Energy occurs in many types resulting from either biogas production, biohydrogen, or voltage output [20,21]. All energy outputs come from the degradation of organic constituents present in the wastewater.

Training studies should be performed for the available adaptation of fungi strains to reduce the toxicity levels of metals. This training study addresses the possible adaptation of fungi strains to metal stress conditions [27].

Microbial fuel cells (MFCs) are a technology that is able to decrease organic compounds present in wastewater using microbial activity and convert the chemical energy into electrical energy via spontaneous oxidation–reduction mechanisms [26]. MFCs can be considered as a method needed for both energy recovery and pollutant removal in tannery wastewater [28].

MFC technology has been used to treat domestic wastewater, swine wastewater, and wastewater from paper recycling [29,30]. Organically loaded compounds in the paper industry were used as a source of energy using microorganisms in a dual-chamber mi-

crobial fuel cell (MFC) [31]. Studies have shown that the increase in the wastewater ionic conductivity increases the MFC power output. Electrolytic matrices as a common additive to stabilize pH [32,33], boost anodic cell conductivity [34,35], and speed up proton transfer mechanisms [36] were necessary for optimal MFC performance.

Feng et al. [37] showed that the addition of 50 mM of phosphate buffer solution (PBS) increased the power output by 136% to 438 mW/m^2, and 200 mM of PBS increased the power output by 158% to 528 mW/m^2, when treating beer brewery wastewater. Huang and Logan [38] observed that the maximum power densities increased from 144 $mW \times m^{-2}$ to 501 $mW \times m^{-2}$ with 50 mM PBS, and 672 $mW \times m^{-2}$ with 200 mM PBS, when treating paper recycling wastewater. Therefore, it is important to assess the effect of adding electrolytes on energy output.

The novelty of this study was to assess the feasibility of treatment of tannery wastewater using a dual-chamber FFC and observe how to improve the operation via the selection of fungal strain, training of fungal strain, and the effect of electrolytic matrices (PBS and BBS) on FFC performance. The performance is determined via assessing the variations in organic degradation represented in COD, TN elimination, and total chromium removal along with the determination of variation in energy output represented in cell voltage output (V), power density (PD), and current density (CD).

2. Materials and Methods

2.1. Fungal Communities in Tannery Wastewater

The goal of this investigation is to cultivate filamentous fungus from tannery effluent collected from contaminated sites with tannery wastewater—chromium stage—from the Elmontaza Tannery, Ain El Sira, Old Cairo, Egypt, in sterilized glass bottles of 1.5 L capacity, transported to the laboratory in an icebox. In a sterile bottle, the samples collected were combined to form a composite sample, and physicochemical analyses were performed as described in Table 1. After that, samples were diluted in a 1:1 ratio in sterile distilled water. To confirm the presence of fungus in the sample, aliquots of 1.0 mL of diluted material were plated onto potato dextrose agar media (PDA) and malt extract agar media (MEA) plates (triplicates). Because the results from PDA and MEA media are comparable, only the PDA medium was used to calculate colony counts. After three days of incubation at 30 ± 1 °C, developed colonies were isolated, counted, and differentiated to the genus level. Purified isolates were obtained by streaking colonies repeatedly on PDA medium and observed under light microscopy. The relative frequency of occurrence was calculated as the number of species isolated divided by the total number of isolates. The fungal isolates were analyzed for certain morphological studies via an image analysis system using Soft-Imaging GmbH software (analysis Pro ver. 3.0), as well as using the newly introduced Regional Center for Mycology and Biotechnology (RCMB) database management system for *Aspergilli* and *Penicillia* identification at the Regional Center for Mycology and Biotechnology (RCMB), Al-Azhar University, Cairo, Egypt.

Table 1. Physicochemical characteristics of raw tannery wastewater.

	Color (Pt-Co)	pH	TDS (mg/L)	COD (mg/L)	TN (mg/L)	EC ($ms \times cm^{-9}$)	Total Cr (mg/L)
Tannery Wastewater Constituents	836 ± 39	4.12 ± 0.015	$21{,}000 \pm 144.9$	1400 ± 37.4	432 ± 20.8	37.7 ± 6.1	500 ± 22.4

2.2. Training of Fungal Strains on Hexavalent Chromium Solution

The relative toxicity of *A. niger* to chromium ion is apparent at higher concentrations. This experiment demonstrated the capability of *A. niger* to adapt to chromium stress conditions and the availability for use in chromium removal from solutions. *A. niger* was subjected to hexavalent chromium ions in levels ranging from 10 to 100 ppm. The adapted

A. niger strain to hexavalent chromium stress is called the trained strain while the *A. niger* strain without any adaptation to hexavalent chromium stress is called the control strain.

2.3. FFCs Operational Set-Up

Two dual-chamber fungal fuel cells, represented in Figure 1, composed of cubic-shaped organic polymer material were used throughout this study. The anodic chambers and cathodic chambers were separated by a cation exchange membrane (CMI-700S Cation Membrane, Membranes International Inc., Ringwood, NJ, USA), and the effective volumes of anodic chambers and cathodic chambers of MFCs were 1.5 L.

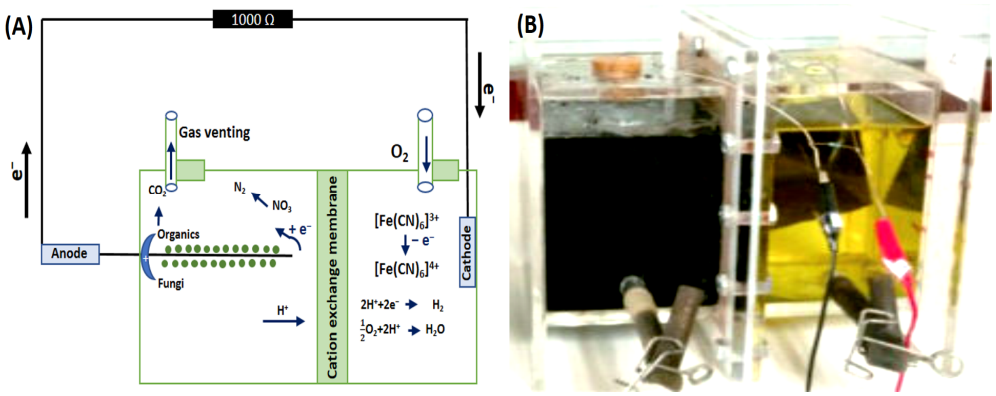

Figure 1. (**A**) Designative scheme of the FFC, and (**B**) lab scale model of the FFC.

Two FFCs were operated in the batch mode in which the anodic chamber was filled with tannery wastewater, 1.5 g/L anhydrous sodium acetate [39], and trained *A. niger* inoculated on a carbon cloth of surface area 64 cm^2 pre-soaked in 15% ethanol for 48 h and heat treated at 450 °C for 1.0 h, as shown in Figure 2 [40]. The anodic chamber of non-electrolytic FFCs does not contain any electrolytes while the electrolytic one contains 50 mM of PBS and 0.2 M of BBS and the anodic pH was adjusted to pH 5.8 [41,42]. The cathodic chamber contains the cathodic redox solutions of 50 mM/L of potassium ferricyanide $K_3[Fe(CN)_6]$ and 50 mM/L PBS [43]. Glass headspace bottles were attached to the top of anodic chambers of FFCs, while the top of headspace bottles were sealed by rubber plugs and penetrated using pinholes, so as to provide an escape passage for nitrogen gas (N_2) generated by reduction of nitrate nitrogen. The cathodes and anodes were connected with titanium wire and an external resistor of 1000 Ω. To determine the internal resistance, different external resistances was used throughout this study. The FFCs were operated for 165 h.

2.4. Analytical Methods

The cell voltage (E, V) was monitored on-line via a data acquisition system (Agilent 34970A; Agilent Technologies, Santa Clara, CA, USA) and recorded automatically every 20 min. The anodic potential (V) was measured against a silver–silver chloride reference electrode (+224.5 mV vs. SHE), which was inserted into the anode chamber. The anodic pH was continuously monitored using a pH meter (PHSJ-5; INESA Instrument, China) and automatically recorded every 30 s. The current (I, A) was calculated according to the following equation [43]:

$$I = \frac{E}{R}$$

where E is cell voltage (V) and R is the external resistance (1000 Ω).

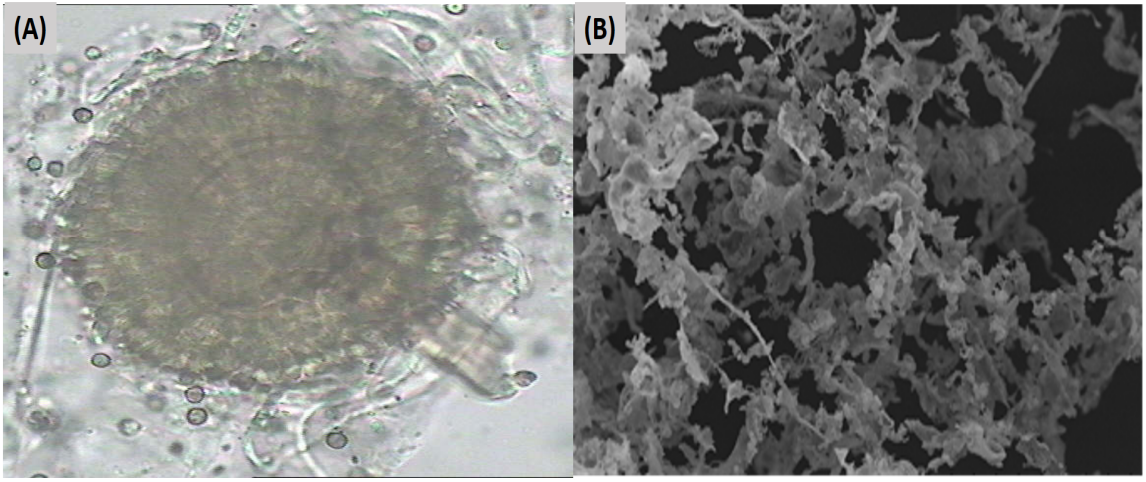

Figure 2. Trained fungal flora inoculated in fungal fuel cells using (**A**) image analysis instrument (mag. 400×) and (**B**) SEM (mag. 40,000×).

The power output of the cells (P, mW) was calculated according to the following equation [43]:

$$P = IE$$

Variable external resistances were used to obtain the polarization curve in which each resistance was changed. Power density (mW/m^2) and current density (mA/m^2) were based on the cathode surface area (m^2) [43].

$$Power\ Density\ (PD) = \frac{U^2}{A * R}$$

$$Current\ Density\ (CD) = \frac{U}{A * R}$$

where U is the voltage output (V), R is the total resistance (Ω) used and A is the electrode area (m^2).

The COD removal efficiency (Ef) % was calculated according to the following equation:

$$Removal\ Efficiency\ (Ef)\ \% = \frac{\Delta S}{S} \times 100$$

where ΔS is the removal of COD concentration (g/L) and S is the initial COD concentration (g/L).

2.5. Statistical Analysis

A linear regression model using "Enter" methods was conducted to evaluate the removal efficiency and predict the estimated removal percent. The statistical program "SPSS 25" was used to determine the histogram and a normal probability plot (P-P plot) of regression.

3. Results and Discussion

3.1. Fungal Communities in Tannery Wastewater

Fifteen fungal colonies representing five genera were obtained on PDA medium at this dilution. Genus *Aspergillus* was found to occur at a maximum percentage (40%), followed by *Penicillium* (26.7%). Genera of *Rhizopus* and *Fusarium* were of a similar percentage (13.3%). Genus *Alternaria* had the minimum percentage (6.7%), as shown in Figure 3.

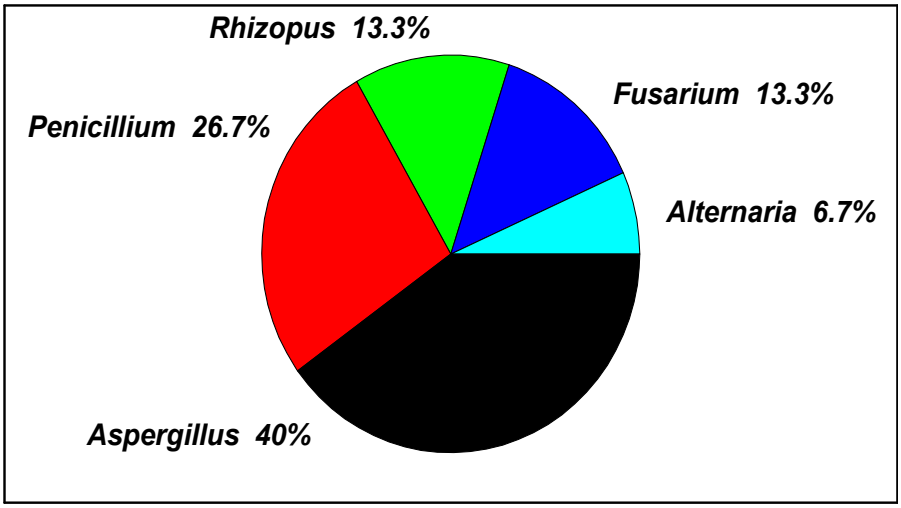

Figure 3. Prevalence of fungal communities in tannery wastewater.

3.2. Training of Fungal Strains on Hexavalent Chromium Solution

The relative toxicity of *A. niger* to hexavalent chromium became obvious at the higher concentration. This test indicated the possible adaptation of *A. niger* to hexavalent chromium stress conditions and their potential for use in extracting metal ions from the solution. Hexavalent chromium is considered one of the most toxic chromium states for microorganisms, so our study focused on measuring the toxicity level of different hexavalent chromium concentrations and the effect of training of the fungal strain on fungal growth rate and adsorption ratio. The *A. niger* strain was trained with high studied hexavalent chromium ion levels ranging from 10 to 100 ppm. A. niger without adaptation to hexavalent chromium stress is called the control strain. The data analysis for biosorption of the studied metal ions by the control and the trained *A. niger* was completed in light of different isothermal models. The results showed that the *A. niger* trained strain had higher maximum removals than the control strain. It also showed that the total growth (G) and the growth rate (μ) of the control and the trained strain were gradually inhibited with an increase in hexavalent chromium concentration, with the control strain being more sensitive as shown in Table 2. In Cr^{6+} assays, the control *A. niger* biotypes grew at 100 ppm with a growth rate of 4.6 mg/h and removal efficiency of 67.5%; meanwhile, the trained strain grew at 100 ppm with a growth rate of 7.3 mg/h and a removal efficiency of 81.8%, as shown in Figures 4 and 5. Further studies are recommended for evaluation of post-treatment and disposal of the Cr-adsorbed fungal strain as a final bio-waste product.

Table 2. Control and trained *A. niger* strain growth behavior under different hexavalent chromium stress conditions.

Cr^{6+}Conc., (mg/L)	Trained Strain			Control Strain		
	Total Growth (G), (mg/L)	Growth Rate (μ), (mg/h)	Cr^{6+} Removed, (%)	Total Growth (G), (mg/L)	Growth Rate (μ), (mg/h)	Cr^{6+} Removed, (%)
0	5600 ± 74.8	33.3 ± 5.8	---	5600 ± 74.8	33.3 ± 5.8	----
10	5420 ± 73.6	32.3 ± 5.7	97.0	5000 ± 70.7	29.8 ± 5.5	88.0
25	5030 ± 70.9	29.9 ± 5.5	90.8	3950 ± 62.8	23.5 ± 4.8	81.6
50	4100 ± 64.0	24.4 ± 4.9	87.2	3000 ± 54.8	17.9 ± 4.2	76.4
75	3200 ± 56.6	19.0 ± 4.4	84.8	1970 ± 44.4	11.7 ± 3.4	72.1
100	1220 ± 34.9	7.3 ± 2.7	81.8	780 ± 27.9	4.6 ± 2.1	67.5

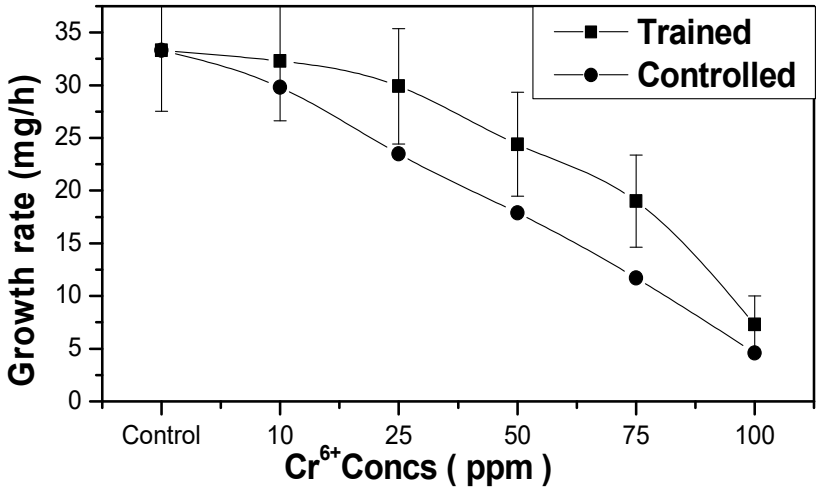

Figure 4. Control and trained *A. niger* strains growth behavior under different hexavalent chromium initial concentrations.

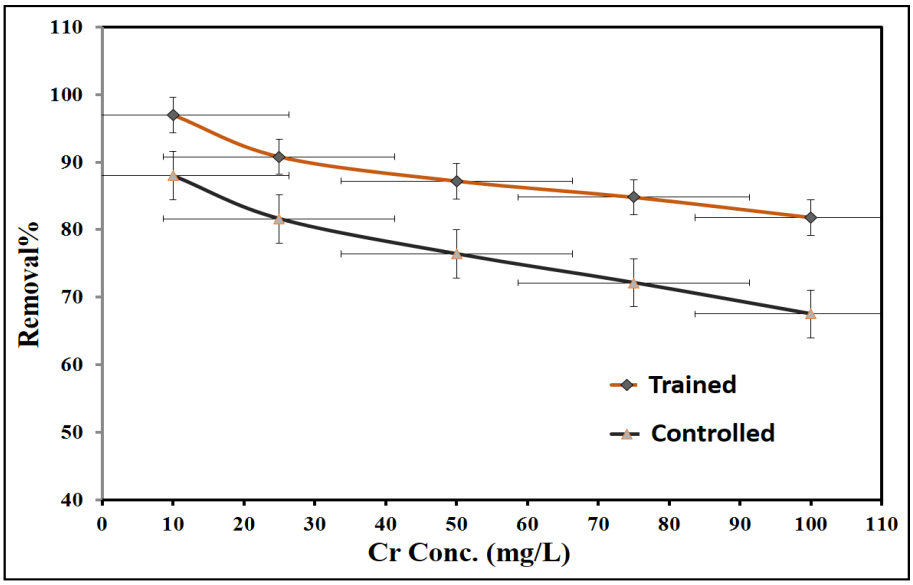

Figure 5. Hexavalent chromium removal efficiency by both the control and trained *A. niger*.

3.3. Adsorption Isotherm

The most common models representing the isotherm behavior for hexavalent chromium sorption in both the trained and control strains were examined, as shown in Figure 6. The findings showed that the Freundlich and Koble–Corrigan models, respectively, can adequately describe the hexavalent chromium sorption in both the trained and control strains. The Freundlich adsorption model can be used to explain heterogeneous adsorption surfaces. The Freundlich isotherm model can also be used to describe multilayer adsorption since it is not limited to monolayer creation. The total amount of materials adsorbed at each particular active site equals the number of molecules that have been adsorbed. The mechanism of the adsorption process depends on the energy of binding between the sorbent and the adsorbed molecules. The adsorption energy progressively dropped until it disappeared after the adsorption process was finished. The three-parameter Koble–Corrigan model, where A, B, and n are Koble–Corrigan constants, combines the Langmuir, Freundlich, and pure hydrocarbon adsorption isotherm models with other adsorption isotherm models [44,45].

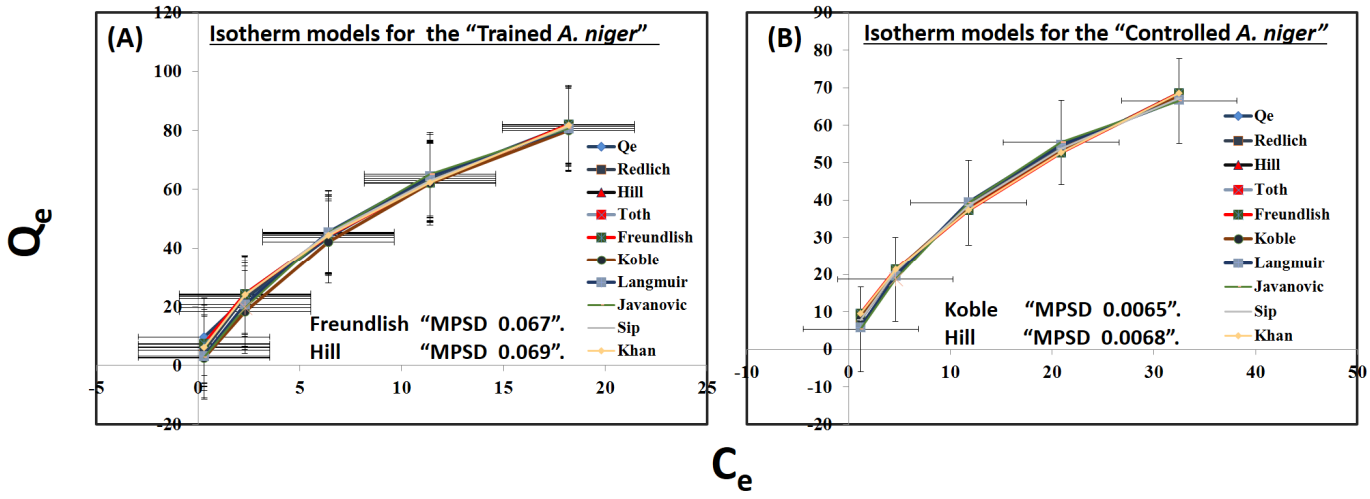

Figure 6. Isotherm models for Cr^{6+} removal by the control and trained strain.

According to the Freundlich model, the maximum uptake of the trained sample was K_f was 14.81 mg/g and n was 1.694. According to the Koble–Corrigan model for the control samples, the maximum uptake was 7.388 mg/g, B was 0.037, and D was 0.755, which showed greater decreases in the uptake values than in the trained sample. The obtained results indicated that the maximum uptake of the trained samples is more efficient than the control samples. Table 3 indicates the variations between experimental and calculated Q_e during isotherm studies for all concentrations.

Table 3. Experimental and calculated Q_e during hexavalent chromium isotherm studies for both the control and trained *A. niger* strains.

A. niger	Q_e	Redlich	Hill	Toth	Freundlich	Koble	Langmuir	Sip	Khan	Javanovic
Trained	9.7	5.2	7.2	7.2	7.3	2.6	3.1	6.3	6.1	2.8
	22.7	23.4	24.2	24.2	24.2	18.2	20.7	23.8	24.0	19.6
	43.6	44.8	44.4	44.4	44.3	42.1	45.5	44.9	44.4	45.2
	63.6	62.9	62.4	62.4	62.3	62.1	64.6	62.9	62.3	65.2
	81.8	81.8	82.1	82.1	82.1	80.1	80.7	81.3	81.9	80.6
Control	8.8	8.0	9.4	5.9	9.5	8.1	5.9	7.8	9.5	5.4
	20.4	21.0	21.2	19.7	21.3	20.9	19.7	20.9	21.3	18.7
	38.2	38.5	37.5	39.4	37.4	38.4	39.4	38.6	37.4	39.3
	54.1	53.6	52.8	54.7	52.7	53.6	54.7	53.7	52.7	55.4
	67.5	67.8	68.5	66.7	68.6	67.6	66.7	67.2	68.6	66.5

3.4. FFC Performance

In two studied FFCs, operations were studied for a treatment time of 165 h. Along with different external resistances ranging from 10 to 20,000 Ω, the internal resistance decreased in the electrolytic cell reaching 65 Ω while the non-electrolytic one was 110 Ω. For an external resistance 1000 Ω and time interval from 15 h to 165 h, the energy output of the electrolytic cell showed an obvious increase compared to the non-electrolytic one. The voltages and power output were gradually decreased along with time according to substrate availability and the level of oxidation/reduction reactions until the power output became stable at 165 h of operation, as shown in Table 4. The rate of decrease in the electrolytic cell was less than that of non-electrolytic cell due to the presence of electrolytes, and in accordance with the change in voltage [46]. The decreasing rate of power activity showed an increase after 90 h for the non-electrolytic cell while it was after 105 h for the electrolytic cell. At 105 h of operation, the electrolyte FFC had a voltage output of 0.613 V, PD of 0.055 mW × m^{-2}, and CD of about 0.089 mA × m^{-2} while the non-electrolyte FFC

had voltage output 0.482 V, PD of 0.032 mW × m^{-2}, and CD of 0.067 mA × m^{-2}. At 165 h of operation, the electrolyte FFC had a voltage output of 0.106 V, PD of 0.0016 mW × m^{-2}, and CD of about 0.015 mA × m^{-2}, while the non-electrolyte FFC had a voltage output of 0.063 V, PD of 0.0005 mW × m^{-2}, and CD of 0.008 mA × m^{-2}. Therefore, the use of electrolytes increases the fungal fuel cell (FFC) performance in terms of power activity and output cell voltages.

Table 4. Variation of energy production of both electrolytic and non-electrolytic FFC.

Time/h	CD/mA·m^{-2}		PD/mW·m^{-2}		U/V	
	Non-Electrolytic FFC	Electrolytic FFC	Non-Electrolytic FFC	Electrolytic FFC	Non-Electrolytic FFC	Electrolytic FFC
0	0	0	0	0	0	0
15	0.1061	0.1194	0.0800	0.0972	0.754	0.814
30	0.1050	0.1165	0.0783	0.0925	0.746	0.794
45	0.1042	0.1150	0.0771	0.0902	0.740	0.784
60	0.1011	0.1127	0.0726	0.0865	0.718	0.768
75	0.0957	0.1086	0.0651	0.0803	0.680	0.740
90	0.0892	0.1046	0.0566	0.0746	0.634	0.713
105	0.0678	0.0899	0.0327	0.0551	0.482	0.613
120	0.0508	0.0704	0.0183	0.0338	0.361	0.480
135	0.0338	0.0506	0.0081	0.0175	0.240	0.345
150	0.0165	0.0276	0.0019	0.0052	0.117	0.188
165	0.0089	0.0156	0.0006	0.0016	0.063	0.106

After 15 h of operation, the FFC voltage outputs were measured and the internal resistance was determined via applying various external resistances ranging from 10 to 20,000 Ω. FFCs voltage, current density showed a relationship, and the line slope led to internal resistance [47]. According to our findings, electrolytic FFCs had internal resistances of just 65 Ω, whereas non-electrolytic FFCs had an internal resistances of 110 Ω.

In addition to the power output, the COD, total nitrogen, and total chromium removal efficiency were examined in both FFCs, as shown in Figure 7. In the anode part, sodium acetate and organic substances present in tannery wastewater were oxidized to CO_2 using fungal strain enzymes. The change in COD consumption for the studied FFCs during the anodic oxidation reduction reaction, organic consumption represented in COD and total nitrogen were consumed, and an increase in power generation and energy output, especially in the electrolytes containing FFCs, occurred [48]. The results showed that at 165 h, electrolytes contained in the FFCs had high COD, total nitrogen, and total chromium removal efficiencies which were 77.9%, 94.2%, and 73.0%, respectively, while non-electrolytes containing FFCs had COD, total nitrogen, and total chromium removal efficiencies of 75.0%, 93.1%, and 61.0%, respectively, due to generation of OH^-, CO_3^{2-}, and HCO_3^- in the electrolyte FFCs resulting from the difference in anodic redox reaction mechanisms and microbial metabolism [49,50]. This variation may be due to the electrolyte energy used in oxidation reduction reactions resulting from acetate and electrolyte materials that increase the electron production from the metabolic activity needed for organic and inorganic degradation to the external circuit of the cell, then to the cathode electron acceptor electrode.

The increase in power output due to the increase in hydroxyl groups in the anode chamber, due to the decrease in organic consumption and the oxidation–reduction reaction rate, gradually decreased [51] due to oxidation of sodium acetate and the presence of the phosphate buffer, resulting in a decrease in cell voltage [52].

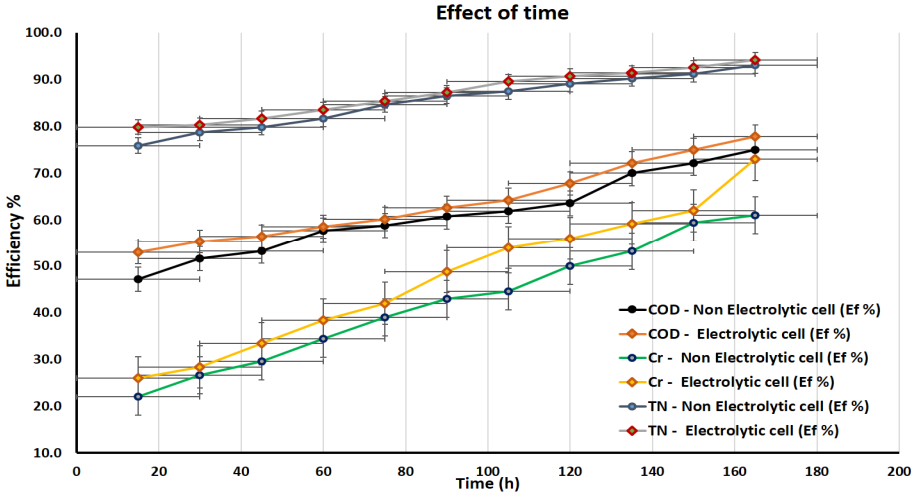

Figure 7. Variation of electrolytic and non-electrolytic FFC treatment performance.

3.5. Statistical Analysis

The statistical analysis was performed using a linear regression model. The obtained results indicated that the R^2 of all parameters lies between 97.0 (COD removal in a non-electrolytic cell) and 99.9% (COD removal in an electrolytic cell), which indicates the success of the model to describe the removal performances, and means that the electrolytic cell is preferred for the degradation of a wide range of organic carbon contaminants in excess of the nitrogen and heavy metal removal as described in the previous discussion. Also, the performance of the model using significance values indicated that, in fact, all models successfully described the removal percentages with a *p*-value < 0.001. Furthermore, the significance results indicated that the time parameter is the most important factor affecting the removal efficiency in the presence of produced energy potential. Finally, the statistical model describes the expected removal percentages depending on time after removing X_2 (volt) shown in Table 5.

Table 5. Regression model for COD, Cr, and TN for electrolytic and non-electrolytic fungal fuel cells.

	Regression Model Electrolytic Cell Model Summary			**Non-Electrolytic Cell Model Summary**		
Method	Enter					
Variables	Time, and Volt					
Dependent	COD	Cr	TN	COD	Cr	TN
R	0.999	0.993	0.995	0.988	0.998	0.998
R^2	0.998	0.985	0.990	0.976	0.996	0.995
Adjusted R^2	0.997	0.982	0.987	0.970	0.994	0.994
Std. error of the estimate	0.426	2.028	0.579	1.502	0.978	0.428
	ANOVA					
Significance	<0.001	<0.001	<0.001	<0.001	<0.001	<0.001
F	1910	269	384	165	895	857
	Coefficient					
Time "Beta"	0.099	0.315	0.116	0.166	0.271	0.152
Time "t"	13.2	8.785	11.317	5.332	13.409	17.111
Time "Significance"	<0.001	<0.001	<0.001	<0.001	<0.001	<0.001
Volt "Beta"	−13.6	3.292	2.905	−1.537	1.682	7.830
Volt "t"	−9.361	0.475	1.470	−0.264	0.444	4.712
Volt "Significance"	<0.001	0.647	0.180	0.799	0.669	0.002
	Estimated removal Equation					
COD removal Eqn.	$\% = 62.8 + 0.099X_1 - 13.596X_2$			$\% = 46.922 + 0.166X_1 - 1.537X_2$		
Cr removal Eqn.	$\% = 17.1 + 0.315X_1 + 3.2926X_2$			$\% = 16.795 + 0.271X_1 + 1.6826X_2$		
TN removal Eqn.	$\% = 74.857 + 0.116X_1 + 2.905X_2$			$\% = 67.736 + 0.152X_1 + 7.830X_2$		

Where X_1 is Time, and X_2 is Volt.

Supplementary: Figures S1–S3, describe the variation between electrolytic and non-electrolytic fungal fuel cells for COD, Cr, and TN removals. The obtained results indicate that the electrolytic cell is more close to linearity with minimum suggestive errors.

4. Conclusions

In the present study, tannery effluents were subjected to treatment using FFCs for organic degradation and energy production. The genus *Aspergillus* represents 40% of the total genera present in tannery wastewater. *A. niger*, which had been subjected to hexavalent chromium stress in the training method, had a faster growth rate (μ) about 7.3 ± 2.7 mg $\times$ h^{-1} and a high hexavalent chromium removal efficiency, reaching 81.8% compared with the control strain. Freundlich and Koble–Corrigan isothermal adsorption models can adequately explain the sorption of hexavalent chromium in both the trained and the control strains. For 165 h of operation, FFC electrolytic matrices showed high energy output represented in output cell voltage output (V), power density (PD), and current density (CD) due to the lower internal resistance compared to the non-electrolytic FFCs. The maximum power output occurred at 15 h of operation, then decreased gradually due to the cell substrate depletion. The electrolytic FFCs also showed high removal efficiencies that reached 77.9%, 94.2%, and 73.0%, in the case of COD, TN, and total chromium, respectively, compared to the non-electrolytic FFC. According to the findings of using FFCs, the trained *A. niger* strain increased the sorption ratio of total chromium and increased the fungal growth rate. Using electrolytic matrices increased the FFC performance that was represented by high energy production and high removal efficiency. Further studies are recommended for the evaluation of post-treatment and disposal of Cr-adsorbed fungal strains as a final bio-waste product.

Supplementary Materials: The following supporting information can be downloaded at: https://www.mdpi.com/article/10.3390/app131910710/s1, Figure S1: Electrolytic and non-electrolytic FFCs treatment performance of COD; Figure S2: Electrolytic and non-electrolytic FFCs treatment performance of Cr; Figure S3: Electrolytic and non-electrolytic FFCs treatment performance of TN.

Author Contributions: Conceptualization, M.S.M., J.-H.W., Y.S., Z.-W.G., A.S.M. and M.K.M.; data curation, M.S.M., J.-H.W., Y.S., Z.-W.G., A.S.M. and M.K.M.; formal analysis, M.S.M., J.-H.W., Y.S., Z.-W.G., A.S.M., M.K.M., R.W.P. and D.-C.Z.; funding acquisition M.S.M., J.-H.W., Y.S. and Z.-W.G.; investigation, M.S.M., J.-H.W., Y.S., Z.-W.G., A.S.M., M.K.M. and R.W.P.; methodology, M.S.M., J.-H.W., Y.S., Z.-W.G., A.S.M., M.K.M. and D.-C.Z.; project administration, M.S.M., J.-H.W., Y.S., Z.-W.G. and Y.Y.; software, M.S.M., J.-H.W., Y.S., Z.-W.G., A.S.M. and M.K.M.; supervision, M.S.M., J.-H.W., Y.S. and Z.-W.G.; validation, M.S.M., J.-H.W., Y.S., Z.-W.G., A.S.M. and M.K.M.; visualization, M.S.M., J.-H.W., Y.S., Z.-W.G., A.S.M., M.K.M., R.W.P., D.-C.Z. and Y.Y.; writing—original draft, M.S.M., J.-H.W., Y.S., Z.-W.G., A.S.M. and M.K.M.; writing—review and editing, M.S.M., J.-H.W., Y.S., Z.-W.G., A.S.M., M.K.M., R.W.P. and Y.Y. All authors have read and agreed to the published version of the manuscript.

Funding: This research was funded by the Talented Young Scientists Program (Egypt-19-069), the Innovation Group of New Technologies for Industrial Pollution Control of Chongqing Education Commission (CXQT19023), the project of Chongqing Technology and Business University (1853061), and Science and Technology Research Project of Chongqing Municipal Education Commission (KJZD-M202000801).

Institutional Review Board Statement: Not applicable.

Informed Consent Statement: Not applicable.

Data Availability Statement: Not applicable.

Acknowledgments: The authors acknowledge all partners of the CTBU, IES-Arish University, BUC, HBRC, UAB, and ERU for support. The authors also acknowledge Xin Yu, the National Research Base of Intelligent Manufacturing Service, Chongqing Technology and Business University, for her contribution throughout the research work.

Conflicts of Interest: The authors declare no conflict of interest.

References

1. Lefebvre, O.; Moletta, R. Treatment of organic pollution in industrial saline wastewater: A literature review. *Water Res.* **2006**, *40*, 3671–3682. [CrossRef] [PubMed]
2. Fei, Y.; Liu, C. Detoxification and resource recovery of chromium-containing wastes. In *Environmental Materials and Waste*; Elsevier: Amsterdam, The Netherlands, 2016; pp. 265–284.
3. Forbes, R.J. *Studies in Ancient Technology Vol V*; Brill Archive: Leiden, The Netherlands, 1966.
4. Sreeram, K.; Ramasami, T. Sustaining tanning process through conservation, recovery and better utilization of chromium. *Resour. Conserv. Recycl.* **2003**, *38*, 185–212. [CrossRef]
5. Gupta, V.K.; Gupta, M.; Sharma, S. Process development for the removal of lead and chromium from aqueous solutions using red mud—An aluminium industry waste. *Water Res.* **2001**, *35*, 1125–1134. [CrossRef] [PubMed]
6. Kurniawan, A.; Sisnandy, V.O.A.; Trilestari, K.; Sunarso, J.; Indraswati, N.; Ismadji, S. Performance of durian shell waste as high capacity biosorbent for Cr (VI) removal from synthetic wastewater. *Ecol. Eng.* **2011**, *37*, 940–947. [CrossRef]
7. Chowdhury, M.; Mostafa, M.; Biswas, T.K.; Saha, A.K. Treatment of leather industrial effluents by filtration and coagulation processes. *Water Resour. Ind.* **2013**, *3*, 11–22. [CrossRef]
8. Szpyrkowicz, L.; Kaul, S.N.; Neti, R.N.; Satyanarayan, S. Influence of anode material on electrochemical oxidation for the treatment of tannery wastewater. *Water Res.* **2005**, *39*, 1601–1613. [CrossRef] [PubMed]
9. Umar, M.; Yusuf, G.; Yaya, A.; Bello, H.; Uwakwe, V.; Mohammed, I.; Tashi, U. Comparative analysis and quality assessment of treated and untreated tannery effluents discharged from NILEST Tannery, Zaria, Kaduna, Nigeria. *Int. J. Sci. Res. Eng. Stud. IJSRES* **2016**, *3*, 29–34.
10. Appiah-Brempong, M.; Essandoh, H.M.K.; Asiedu, N.Y.; Dadzie, S.K.; Momade, F.W.Y. Artisanal tannery wastewater: Quantity and characteristics. *Heliyon* **2022**, *8*, e08680. [CrossRef]
11. Lefebvre, O.; Habouzit, F.; Bru, V.; Delgenès, J.-P.; Godon, J.-J.; Moletta, R. Treatment of hypersaline industrial wastewater by a microbial consortium in a sequencing batch reactor. *Environ. Technol.* **2004**, *25*, 543–553. [CrossRef]
12. Vidal, G.; Aspé, E.; Marti, M.C.; Roeckel, M. Treatment of recycled wastewaters from fishmeal factory by an anaerobic filter. *Biotechnol. Lett.* **1997**, *19*, 117–122. [CrossRef]
13. Roeckel, M.; Aspé, E.; Martí, M.C. Achieving clean technology in the fish-meal industry by addition of a new process step. *J. Chem. Technol. Biotechnol. Int. Res. Process Environ. Clean Technol.* **1996**, *67*, 96–104. [CrossRef]
14. Li, H.; Zhou, B.; Tian, Z.; Song, Y.; Xiang, L.; Wang, S.; Sun, C. Efficient biological nitrogen removal by Johannesburg-Sulfur autotrophic denitrification from low COD/TN ratio municipal wastewater at low temperature. *Environ. Earth Sci.* **2015**, *73*, 5027–5035. [CrossRef]
15. Karam, A.; Mostafa, M.; Elawwad, A.; Zaher, K.; Mahmoud, A.S.; Peters, R. Small-pilot plant for tertiary treatment of domestic wastewater using algal photo-bioreactor, with artificial intelligence. In Proceedings of the 2019 AIChE Annual Meeting, Orlando, FL, USA, 13 November 2019.
16. Kundu, D.; Dutta, D.; Samanta, P.; Dey, S.; Sherpa, K.C.; Kumar, S.; Dubey, B.K. Valorization of wastewater: A paradigm shift towards circular bioeconomy and sustainability. *Sci. Total Environ.* **2022**, *848*, 157709. [CrossRef] [PubMed]
17. Mahmoud, A.S. Effect of nano bentonite on direct yellow 50 dye removal; Adsorption isotherm, kinetic analysis, and thermodynamic behavior. *Prog. React. Kinet. Mech.* **2022**, *47*, 14686783221090377. [CrossRef]
18. Lefebvre, O.; Vasudevan, N.; Torrijos, M.; Thanasekaran, K.; Moletta, R. Halophilic biological treatment of tannery soak liquor in a sequencing batch reactor. *Water Res.* **2005**, *39*, 1471–1480. [CrossRef] [PubMed]
19. Heberling, J.; Adewuyi, Y.; Mahmoud, A.S.; Mostafa, M.; Peters, R.W. AOP Performance at Wastewater Treatment Plants. In Proceedings of the 2018 Annual AIChE Meeting, Pittsburgh, PA, USA, 28 October–2 November 2018.
20. Naguib, A.M.; Abdel-Gawad, S.A.; Mostafa, M.K.; Peters, R.W.; Mahmoud, A.S. Critical Review of the Fenton Oxidation Process for Industrial Wastewater Treatment. In Proceedings of the Annual AIChE Meeting, Phoenix, AZ, USA, 13–18 November 2022; pp. 1–9.
21. Ellouze, E.; Amar, R.B.; Boufi, S.; Salah, A. Coagulation-flocculation performances for cuttlefish effluents treatment. *Environ. Technol.* **2003**, *24*, 1357–1366. [CrossRef] [PubMed]
22. Bae, B.-U.; Jung, Y.-H.; Han, W.-W.; Shin, H.-S. Improved brine recycling during nitrate removal using ion exchange. *Water Res.* **2002**, *36*, 3330–3340. [CrossRef] [PubMed]
23. Afonso, M.D.; Borquez, R. Review of the treatment of seafood processing wastewaters and recovery of proteins therein by membrane separation processes—Prospects of the ultrafiltration of wastewaters from the fish meal industry. *Desalination* **2002**, *142*, 29–45. [CrossRef]
24. Church, J.; Hwang, J.-H.; Kim, K.-T.; McLean, R.; Oh, Y.-K.; Nam, B.; Joo, J.C.; Lee, W.H. Effect of salt type and concentration on the growth and lipid content of Chlorella vulgaris in synthetic saline wastewater for biofuel production. *Bioresour. Technol.* **2017**, *243*, 147–153. [CrossRef]
25. Jang, D.; Hwang, Y.; Shin, H.; Lee, W. Effects of salinity on the characteristics of biomass and membrane fouling in membrane bioreactors. *Bioresour. Technol.* **2013**, *141*, 50–56. [CrossRef]
26. Wang, X.; Cheng, S.; Zhang, X.; Li, X.-Y.; Logan, B.E. Impact of salinity on cathode catalyst performance in microbial fuel cells (MFCs). *Int. J. Hydrogen Energy* **2011**, *36*, 13900–13906. [CrossRef]
27. Malik, A. Metal bioremediation through growing cells. *Environ. Int.* **2004**, *30*, 261–278. [CrossRef] [PubMed]

28. You, S.J.; Zhang, J.N.; Yuan, Y.X.; Ren, N.Q.; Wang, X.H. Development of microbial fuel cell with anoxic/oxic design for treatment of saline seafood wastewater and biological electricity generation. *J. Chem. Technol. Biotechnol.* **2010**, *85*, 1077–1083. [CrossRef]
29. Logan, B.E.; Rabaey, K. Conversion of wastes into bioelectricity and chemicals by using microbial electrochemical technologies. *Science* **2012**, *337*, 686–690. [CrossRef]
30. Fan, Y.; Hu, H.; Liu, H. Enhanced Coulombic efficiency and power density of air-cathode microbial fuel cells with an improved cell configuration. *J. Power Sources* **2007**, *171*, 348–354. [CrossRef]
31. Karuppiah, T.; Uthirakrishnan, U.; Sivakumar, S.V.; Authilingam, S.; Arun, J.; Sivaramakrishnan, R.; Pugazhendhi, A. Processing of electroplating industry wastewater through dual chambered microbial fuel cells (MFC) for simultaneous treatment of wastewater and green fuel production. *Int. J. Hydrogen Energy* **2022**, *47*, 37569–37576. [CrossRef]
32. Lefebvre, O.; Tan, Z.; Kharkwal, S.; Ng, H.Y. Effect of increasing anodic NaCl concentration on microbial fuel cell performance. *Bioresour. Technol.* **2012**, *112*, 336–340. [CrossRef] [PubMed]
33. Gil, G.-C.; Chang, I.-S.; Kim, B.H.; Kim, M.; Jang, J.-K.; Park, H.S.; Kim, H.J. Operational parameters affecting the performannce of a mediator-less microbial fuel cell. *Biosens. Bioelectron.* **2003**, *18*, 327–334. [CrossRef]
34. Logan, B.; Cheng, S.; Watson, V.; Estadt, G. Graphite fiber brush anodes for increased power production in air-cathode microbial fuel cells. *Environ. Sci. Technol.* **2007**, *41*, 3341–3346. [CrossRef]
35. Prathiba, S.; Kumar, P.S.; Vo, D.V. Recent advancements in microbial fuel cells: A review on its electron transfer mechanisms, microbial community, types of substrates and design for bio-electrochemical treatment. *Chemosphere* **2022**, *286*, 131856. [CrossRef]
36. Nam, J.-Y.; Kim, H.-W.; Lim, K.-H.; Shin, H.-S.; Logan, B.E. Variation of power generation at different buffer types and conductivities in single chamber microbial fuel cells. *Biosens. Bioelectron.* **2010**, *25*, 1155–1159. [CrossRef] [PubMed]
37. Feng, Y.; Wang, X.; Logan, B.E.; Lee, H. Brewery wastewater treatment using air-cathode microbial fuel cells. *Appl. Microbiol. Biotechnol.* **2008**, *78*, 873–880. [CrossRef] [PubMed]
38. Huang, L.; Logan, B.E. Electricity generation and treatment of paper recycling wastewater using a microbial fuel cell. *Appl. Microbiol. Biotechnol.* **2008**, *80*, 349–355. [CrossRef] [PubMed]
39. Balch, W.; Fox, G.E.; Magrum, L.J.; Woese, C.R.; Wolfe, R. Methanogens: Reevaluation of a unique biological group. *Microbiol. Rev.* **1979**, *43*, 260–296. [CrossRef] [PubMed]
40. Jayashree, R.S.; Egas, D.; Spendelow, J.S.; Natarajan, D.; Markoski, L.J.; Kenis, P.J.; Letters, S.-S. Air-breathing laminar flow-based direct methanol fuel cell with alkaline electrolyte. *Electrochem. Solid-State Lett.* **2006**, *9*, A252. [CrossRef]
41. Ambler, J.R.; Logan, B.E. Evaluation of stainless steel cathodes and a bicarbonate buffer for hydrogen production in microbial electrolysis cells using a new method for measuring gas production. *Int. J. Hydrogen Energy* **2011**, *36*, 160–166. [CrossRef]
42. Fan, Y.; Hu, H.; Liu, H. Sustainable power generation in microbial fuel cells using bicarbonate buffer and proton transfer mechanisms. *Environ. Sci. Technol.* **2007**, *41*, 8154–8158. [CrossRef]
43. Liu, H.; Ramnarayanan, R.; Logan, B.E. Production of electricity during wastewater treatment using a single chamber microbial fuel cell. *Environ. Sci. Technol.* **2004**, *38*, 2281–2285. [CrossRef]
44. Shahbeig, H.; Bagheri, N.; Ghorbanian, S.A.; Hallajisani, A.; Poorkarimi, S. A new adsorption isotherm model of aqueous solutions on granular activated carbon. *World J. Model. Simul.* **2013**, *9*, 243–254.
45. Mandal, A.; Singh, N.J.; Health, P.B. Kinetic and isotherm error optimization studies for adsorption of atrazine and imidacloprid on bark of *Eucalyptus tereticornis* L. *J. Environ. Sci. Health* **2016**, *51*, 192–203. [CrossRef]
46. Cheng, S.; Liu, H.; Logan, B.E. Power densities using different cathode catalysts (Pt and CoTMPP) and polymer binders (Nafion and PTFE) in single chamber microbial fuel cells. *Environ. Sci. Technol.* **2006**, *40*, 364–369. [CrossRef] [PubMed]
47. Fan, Y.; Sharbrough, E.; Liu, H. Quantification of the internal resistance distribution of microbial fuel cells. *Environ. Sci. Technol.* **2008**, *42*, 8101–8107. [CrossRef] [PubMed]
48. Yuan, Y.; Zhao, B.; Zhou, S.; Zhong, S.; Zhuang, L. Electrocatalytic activity of anodic biofilm responses to pH changes in microbial fuel cells. *Bioresour. Technol.* **2011**, *102*, 6887–6891. [CrossRef] [PubMed]
49. Sukkasem, C.; Xu, S.; Park, S.; Boonsawang, P.; Liu, H. Effect of nitrate on the performance of single chamber air cathode microbial fuel cells. *Water Res.* **2008**, *42*, 4743–4750. [CrossRef] [PubMed]
50. Li, J.-T.; Zhang, S.-H.; Hua, Y.-M. Performance of denitrifying microbial fuel cell subjected to variation in pH, COD concentration and external resistance. *Water Sci. Technol.* **2013**, *68*, 250–256. [CrossRef] [PubMed]
51. Raghavulu, S.V.; Mohan, S.V.; Reddy, M.V.; Mohanakrishna, G.; Sarma, P. Behavior of single chambered mediatorless microbial fuel cell (MFC) at acidophilic, neutral and alkaline microenvironments during chemical wastewater treatment. *Int. J. Hydrogen Energy* **2009**, *34*, 7547–7554. [CrossRef]
52. He, Z.; Huang, Y.; Manohar, A.K.; Mansfeld, F. Effect of electrolyte pH on the rate of the anodic and cathodic reactions in an air-cathode microbial fuel cell. *Bioelectrochemistry* **2008**, *74*, 78–82. [CrossRef]